

Bond Breaking Kinetics in Mechanically Controlled Break Junction Experiments: A Bayesian Approach

Dylan Dyer and Oliver L. A. Monti*



Cite This: *J. Phys. Chem. Lett.* 2023, 14, 10935–10942



Read Online

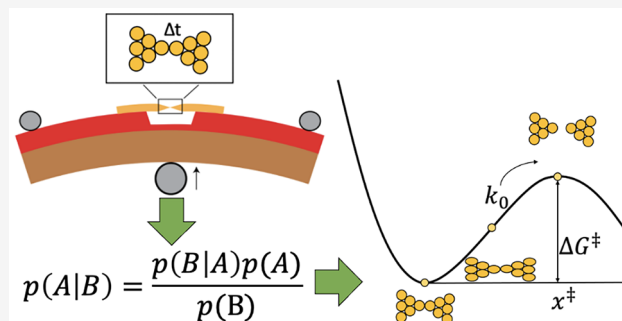
ACCESS |

Metrics & More

Article Recommendations

Supporting Information

ABSTRACT: Break junction experiments allow investigating electronic and spintronic properties at the atomic and molecular scale. These experiments generate by their very nature broad and asymmetric distributions of the observables of interest, and thus, a full statistical interpretation is warranted. We show here that understanding the complete lifetime distribution is essential for obtaining reliable estimates. We demonstrate this for Au atomic point contacts by adopting Bayesian reasoning to make maximal use of all measured data to reliably estimate the distance to the transition state, x^\ddagger , the associated free energy barrier, ΔG^\ddagger , and the curvature, ν , of the free energy surface. Obtaining robust estimates requires less experimental effort than with previous methods and fewer assumptions and thus leads to a significant reassessment of the kinetic parameters in this paradigmatic atomic-scale structure. Our proposed Bayesian reasoning offers a powerful and general approach when interpreting inherently stochastic data that yield broad, asymmetric distributions for which analytical models of the distribution may be developed.



In single-molecule electronics, test beds have been developed to isolate single organic molecules and to characterize their conductance, $G = 1/R$. Charge transport at the nanoscale deviates significantly from Ohm's law because macroscopic diffusive transport shifts into microscopic ballistic transport when length scales are comparable to the de Broglie wavelength. While the linear current–voltage characteristic is still retained at such length scales, it requires the ballistic transport to be treated in the full quantum regime. At this scale, measurements performed in either mechanically controlled break junction (MCBJ) or scanning tunneling microscope–break junction (STM-BJ) experiments yield widely distributed and asymmetric conductance and lifetime histograms for both pure Au and molecular junctions because the measurements are sensitive to the stochastic microscopic detail of junction formation and rupture. How to interpret these distributions and reliably extract the most information is an ongoing challenge because these distributions may contain valuable yet thus far untapped information about the physics of quantum transport in such atomic-scale contacts. Worse, the distributions may obscure the true underlying physics, leading to biased or potentially even wrong conclusions that could stem from previously understood but untreated consequences of the experimental architecture. This prompts the need for microscopic insights into the factors that contribute e.g. to the broad experimental conductance or lifetime histograms, with the aim to invert the distributions into atomistic behavior and properties. This is the fundamental challenge in break junction experiments, where data are usually widely distributed.

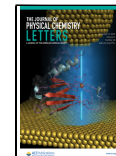
Progress has been made to develop analytical expressions for the conductance histogram in terms of parameters that describe the kinetic profile of the junction and its mechanical manipulation, including the histogram shape. In particular, Mejia and co-workers show that one may derive expressions for the shape of the conductance histograms by considering the statistical mechanics of junction formation and rupture. The microscopic model requires independent force and conductance measurements to extract all physically meaningful parameters but allows a more complete understanding of the conductance histogram.^{1,2} Our approach has the potential to test this work by extracting relevant quantities directly from conductance measurements only and from a single junction, offering the considerable advantage of internal data consistency. Despite these advances in generating possible distributions based on microscopic parameters, inverting experimental distributions to retrieve the underlying model parameters remains a formidable task. The situation is worse for extracting information from lifetime histograms because this has mostly been limited to single point measures, such as the mean or most likely value.

Received: September 19, 2023

Revised: November 20, 2023

Accepted: November 27, 2023

Published: November 30, 2023



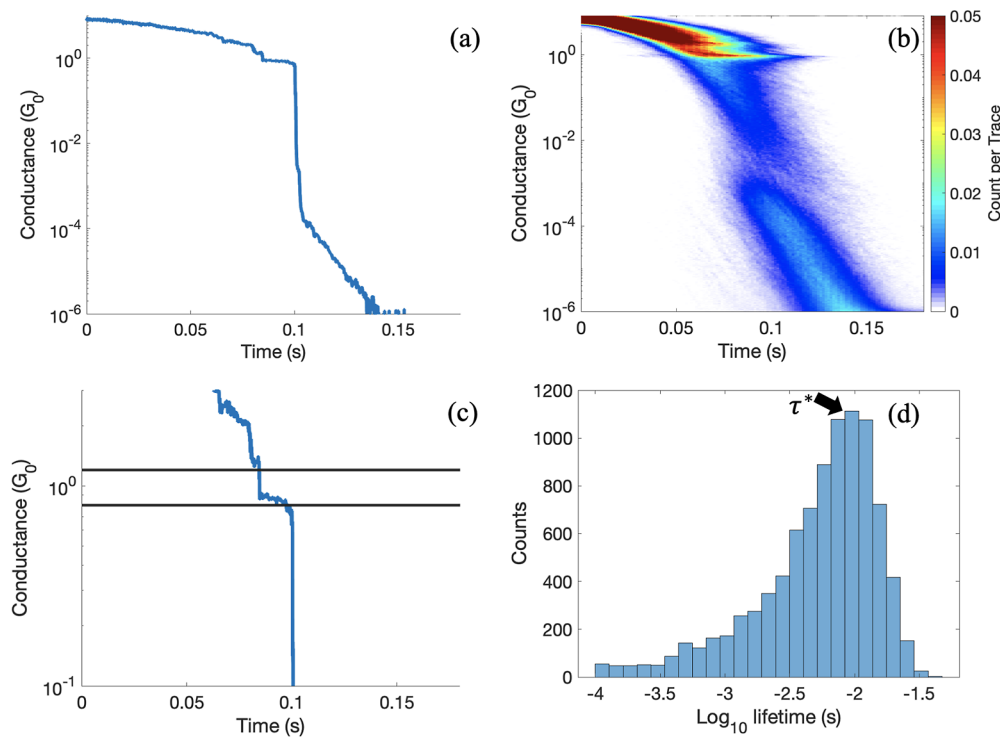


Figure 1. (a) Example conductance–time “trace” of one stretching cycle in our break junction experiment. (b) Aggregate data of thousands of conductance–time “traces” in a 2D-conductance–time histogram. (c) Zoomed-in conductance–time “trace” displaying the quantized steps in conductance when the contact area of the wire is only a few atoms wide, with a conductance window drawn from 0.8 to 1.2 G_0 . (d) 1D-lifetime histogram near 1 G_0 , with the most probable lifetime, τ^* , indicated by the black arrow.

Here we show that kinetic parameters for bond breaking obtained in this manner need to be reassessed. To achieve this, we employ an effective one-dimensional fully microscopic model developed by Dudko et al. for force experiments on biomolecules to capture all relevant kinetic aspects of bond breaking in the junction.³ We will later describe different models used and compare our findings to these and previous reports based on these. Inverting the experimental lifetime distributions allows us thus for the first time with minimal auxiliary assumptions to directly assess the rupture kinetics in atomic point contacts and to compare the extracted kinetic parameters to different microscopic models.^{4,5} This opens the door not only for studying bond breaking kinetics at the atomic or potentially single-molecule level but also for helping design improved nanoscale wire constructs that remain stable for extended periods of time, in turn facilitating more complex multiprobe-based break junction experiments. Rather than the standard least-squares method, which requires binning the data, we show that by means of a powerful Bayesian approach we can use *all* the data and therefore the complete experimental shape of the histogram. This allows us to invert the full experimental distribution, providing robust estimates for previously inaccessible kinetic parameters even in cases where standard maximum likelihood estimation (MLE) methods fail and leading us to a reassessment of the free energy for breaking Au–Au bonds. We begin by briefly presenting typical experimental lifetime distributions from Au break junctions and how they are influenced by externally controlled parameters. We then developed the Bayesian framework to extract kinetic parameters for bond breaking in Au junctions and validate our approach. Finally, we discuss the

meaning of the thus retrieved kinetic parameters in light of previous estimates by simpler methods.

In MCBJ experiments, an electrical bias is applied across a metallic wire. This Au wire is then stretched via a piezo motor to the point of rupture, forming a nanoscopic gap between the two electrodes. The electrodes are eventually mechanically pushed back together by reversing the piezo motor extension to reform the wire, and the stretching and reforming processes are repeated. We recorded the conductance of these wires as a function of time during the breaking and reforming process. Figure 1a shows a typical example “trace” of one stretching cycle, showing the decreasing conductance with stretching as the wire thins, followed by sudden rupture and eventually exponential decay due to tunneling through the newly formed gap. The general shape of these traces is preserved when the mechanical stretching and reforming cycle is repeated thousands of times. We visualize the aggregate data in a 2D-conductance–time histogram, shown in Figure 1b, clearly highlighting the characteristic behavior (decreasing conductance and then rupture followed by exponential decay) of Au junctions. Zooming in more closely into a single trace, Figure 1c displays well-known quantized steps in conductance when the contact area of the wire is only a few atoms wide. Of specific interest is the amount of time that the contact conductance spends near 1 G_0 (the fundamental quantum of conductance), say within a window from 0.8 to 1.2 G_0 , as shown in Figure 1c. This conductance window corresponds to a monovalent Au–Au contact area of an atomically thin wire just before rupture, and its lifetime describes the electro-mechanical properties of such a Au wire. To understand and interpret these properties, thousands of traces are acquired and their lifetimes near 1 G_0 are collected and binned, shown in

Figure 1d (see the Supporting Information for the effect of changing this window on the estimated parameters).

The characteristically highly asymmetric lifetime histogram may be summarized by identifying e.g. the most probable lifetime (τ^*). This indicates that stable contacts of a particular configuration or at least a particular lifetime are statistically favored to form. However, for a constant stretching speed, the measured certainty in τ^* is low, apparently from observed lifetime values spanning several orders of magnitude, with a tail toward short lifetimes due to rare rupture events caused by thermal fluctuations.⁶ We attribute the shape of the lifetime distribution and the lack of certainty in τ^* to the stochastic nature of the atomic arrangement in the metallic wire during the stretching, rupture, and reforming process and to the fact that Au atoms at room temperature are mobile.⁷

Interestingly, the lifetime distribution shares a similar single peak structure across different stretching speeds. Despite the aforementioned shortcomings, we therefore first consider the most probable lifetime τ^* as a function of junction stretching speed (Figure 2) as a key parameter that may encode the relevant breaking kinetics, as originally proposed by Evans and co-workers.^{8,9}

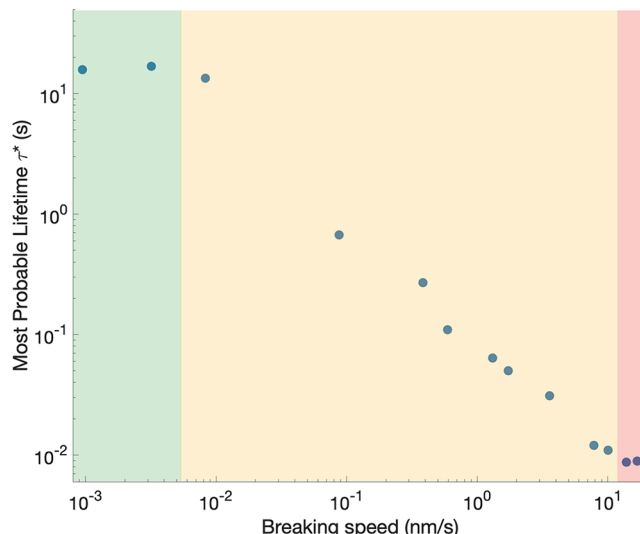


Figure 2. Most probable lifetime τ^* as a function of junction stretching speed. The green segment highlights spontaneous rupture due to thermal fluctuations (speed independent). The yellow segment highlights the mixed spontaneous rupture and force-induced rupture (exponentially dependent on the breaking speed). The red segment highlights instantaneous force-induced rupture (speed independent).

At extremely slow stretching speeds, the most probable lifetime is determined by breaking events caused by spontaneous thermal fluctuations.^{8,9} It is independent of the stretching speed, as highlighted in the green segment of Figure 2. At moderate stretching speeds, the most probable lifetime displays logarithmically linear behavior because the external force increases quickly enough to lower the free energy barrier for rupture before a spontaneous rupture can occur (yellow segment in Figure 2). Finally, at extreme stretching speeds, bond breaking due to spontaneous thermal fluctuations is completely suppressed, and rupture is instead dominated by the applied force. This force rapidly approaches the maximum tensile strength of the bond. This regime is highlighted in the red segment in Figure 2.

While this behavior and the three different regimes are readily understood, it is difficult to obtain robust estimates of the relevant bond breaking parameters from such data. To overcome this hurdle, we take inspiration from the extensive body of work on protein bond rupture kinetics. In an effective one-dimensional microscopic model, Dudko et al. were able to capture all relevant aspects of bond breaking in a simple rate equation³

$$k(F) = k_0 \left(1 - \frac{\nu F x^{\ddagger}}{\Delta G^{\ddagger}}\right)^{(1/\nu)-1} e^{\Delta G^{\ddagger} [1 - (1 - \nu F x^{\ddagger} / \Delta G^{\ddagger})^{1/\nu}]} \quad (1)$$

where $k(F)$ is the rate of rupture of a Au–Au bond as a function of an externally applied force F , k_0 is the intrinsic rate of a Au–Au bond breaking under zero force, x^{\ddagger} is the distance from the free energy minimum to the transition state, ΔG^{\ddagger} is the height of the free energy barrier to be overcome for rupture, and ν is the curvature of the free energy surface. Equation 1 describes both constant-force and time-dependent linear force experiments, allowing both forces and lifetimes to be analyzed by the simple relation $F = KV$, where K is the effective spring constant and V is the stretching speed. We show in the Supporting Information that our MCBJ architecture satisfies force–time linearity. For $\nu = 1$ and $\Delta G^{\ddagger} \rightarrow \infty$ independent of ν , eq 1 reduces to the well-known phenomenological expression by Bell, $k(F) = k_0 e^{F x^{\ddagger} / k_B T}$, where k_B is the Boltzmann constant and T is temperature.⁵ Bell's expression is frequently used to extract from mean rupture force measurements in optical tweezer-single-molecule pulling experiments the intrinsic rate coefficient (k_0) and the distance along the pulling direction between the free-energy minimum and the transition state (x^{\ddagger}).^{8,9} Note that Bell's expression does not allow one to estimate the height or curvature of the free energy barrier and its surface (ΔG^{\ddagger} , ν), which are arguably the most insightful and physically intuitive parameters in the description of the kinetics of bond breaking.

Under the assumptions of the model by Dudko et al., analytical formulas for the mean and variance of the rupture force distribution can be derived. Hummer and Szabo show that if one were to try and extract all three kinetic parameters k_0 , x^{\ddagger} , and ΔG^{\ddagger} (when $\nu = \frac{1}{2}$) by fitting merely the mean forces for a range of stretching speeds from experimental data, then the χ^2 surfaces are marred by highly correlated parameters with large uncertainties in the fit.¹⁰ This situation is analogous to estimating the kinetic parameters for Au junction rupture in atomic point contact experiments. Performing a global fit of mean forces and the variances over all pulling speeds improves the situation, but extracting all three parameters, and most importantly, ΔG^{\ddagger} , remains extremely challenging.

Instead, a statistically much more powerful and sounder approach is to use the entire rupture time distribution. From eq 1 and considering the junction survival probability, Dudko et al. obtained an analytical expression for the lifetime distribution for a constant stretching speed:³

$$p(\tau|V) = k(F(\tau)) e^{k_0 / x^{\ddagger} KV} e^{-[k(F(\tau)) / x^{\ddagger} KV] [1 - (V K V x^{\ddagger} / \Delta G^{\ddagger})]^{1-(1/\nu)}} \quad (2)$$

Because standard MLE techniques either fail or provide poor estimates of the kinetic parameters and because we have a readily accessible if complex parametrized stochastic model for the junction lifetimes in eq 2, we show now that it is natural to adopt Bayesian estimation procedures to extract relevant

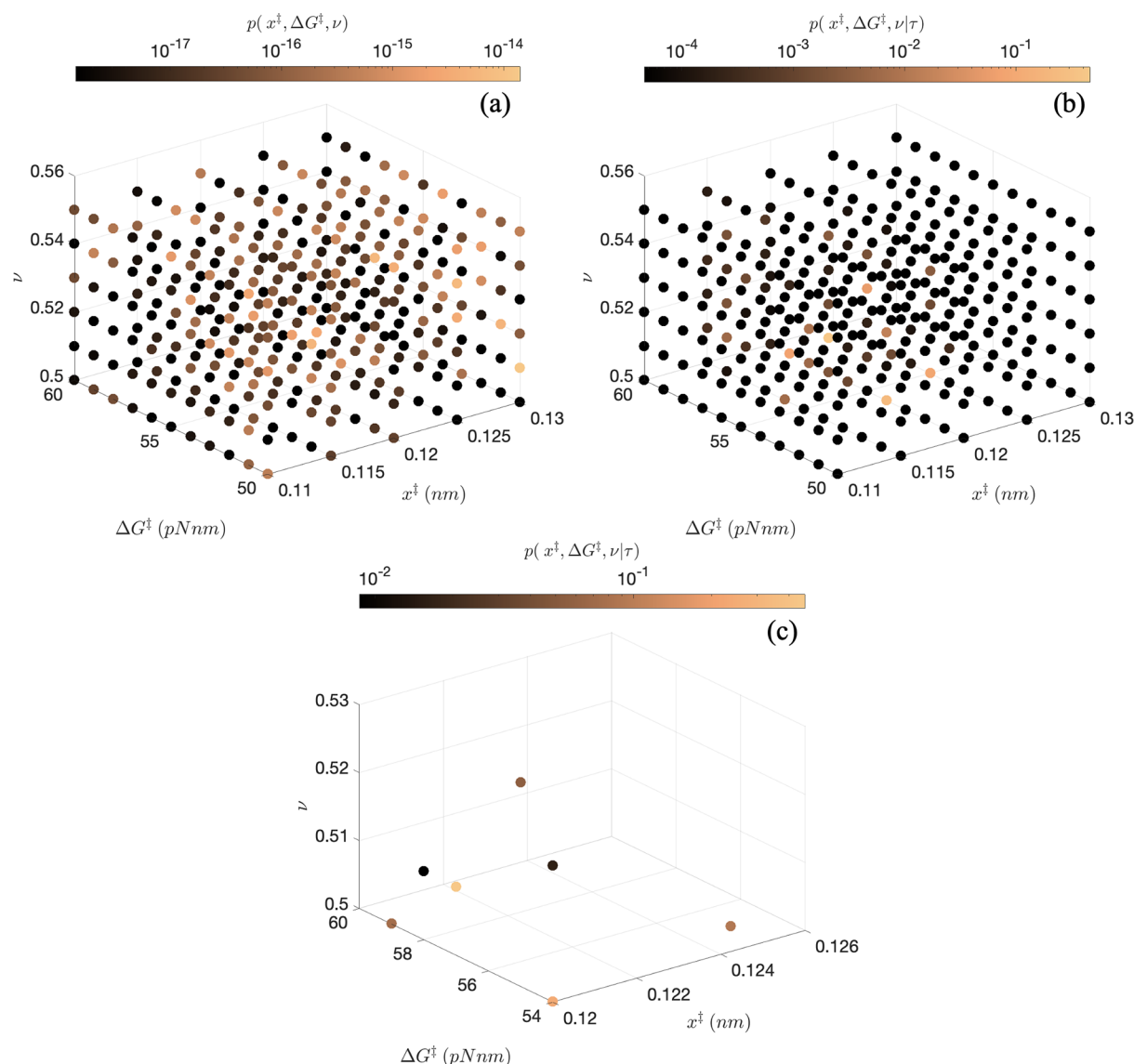


Figure 3. (a) Calculated reference prior distribution which quantifies the amount of expected information in eq 2 into the prior distribution. (b) Full posterior distribution. (c) Calculated density-based 95% credible interval. The breaking speed is 0.65 nm/s, and 160 pN nm = 1 eV.

electromechanical and physically meaningful junction properties. In what follows we demonstrate that such a Bayesian approach has the powerful advantage of making maximal use of *all* the measured data; i.e., unlike MLE, it is not just based on most likely lifetimes or other similar single point measures. This is a central result of our work and leads to a reassessment of key kinetic parameters for bond breaking in the paradigmatic Au nanowires.

Using eq 2 to describe the probability distribution of our experimentally measured lifetimes of monovalent Au–Au contacts, we invoke the Bayes theorem to analytically calculate the posterior probability distribution of the most likely parameter quartet $(k_0, x^{\ddagger}, \Delta G^{\ddagger}, \nu)$ given our experimental data

$$p(k_0, x^{\ddagger}, \Delta G^{\ddagger}, \nu | \tau) = \frac{p(\tau | V) p(k_0, x^{\ddagger}, \Delta G^{\ddagger}, \nu)}{p(\tau)} \quad (3)$$

where $p(\tau | V)$ is the likelihood function, i.e., the mathematical model believed to describe the data, $p(k_0, x^{\ddagger}, \Delta G^{\ddagger}, \nu)$ is the prior distribution which expresses our belief about the probability of the parameter quartet before any evidence is

considered, and $p(\tau)$ is a normalization term. Before the Bayes theorem may be used, two choices must be made. The first is that a prior distribution must be decided on. An unavoidable fact of Bayesian reasoning is that bias will *always* be introduced into the calculation of the posterior when selecting a prior distribution; we emphasize, however, that the explicit nature of stating the bias is one of the advantages of Bayesian statistics over frequentist analysis, where the bias is implicit and not clearly articulated. Considering this, we quantify information on our mathematical model (eq 2) into the prior distribution by adopting the robust reference prior method developed by Berger and Bernardo (see the *Supporting Information* for an outline of how to construct the reference prior).¹¹ The second choice, which is specific to our study, is how to handle k_0 . While it would be ideal to compute the posterior for the quartet of parameters $(k_0, x^{\ddagger}, \Delta G^{\ddagger}, \nu)$, it is more tractable to instead determine k_0 experimentally and then estimate the triplet $(x^{\ddagger}, \Delta G^{\ddagger}, \nu)$. We show in the *Supporting Information* that even when k_0 is varied by a factor of 2, it does not substantially change our estimates of the triplet.

We now use this framework to assess the electromechanical properties of a nanoscale Au wire. We have experimentally measured the inverse of the intrinsic lifetime for which an Au–Au bond will survive under zero force (k_0 , thermally activated rupture) and set that value to be the inverse of the average of the two most probable lifetimes shown in the green region of Figure 2. We then use our Bayesian approach, including a reference prior to this, to estimate x^\ddagger , ΔG^\ddagger , and ν for different breaking speeds. Figure 3 shows an example of the reference prior distribution, the full posterior distribution, and the density based 95% credible interval calculated from the full posterior distribution. The credible interval expresses our uncertainty of the estimated triplet value. Note that the bounds chosen when calculating the prior distribution do not restrict the 95% credible interval, showing that our choice of bounds does not influence the estimation. This is found for all fits investigated. Table 1 summarizes the resulting 95% credible

Table 1. Model Parameters Obtained by Fitting Experimental Lifetime Data with a Reference Prior Distribution^a

experimental condition	95% credible interval		
	x^\ddagger (nm)	ΔG^\ddagger (eV)	ν
0.09	0.050	0.294–0.319	0.52–0.55
0.40	0.075	0.338	0.50–0.52
0.65	0.120–0.125	0.337–0.369	0.50–0.53
1.20	0.120–0.125	0.350–0.369	0.50–0.51
3.80	0.120–0.125	0.381–0.469	0.50–0.55
11.9	0.145–0.150	0.375–0.413	0.50–0.52
15.5	0.135–0.145	0.406–0.438	0.50–0.53

^aA single value reported rather than a range indicates that the uncertainty of the estimate in x^\ddagger is less than 0.05 nm and for ΔG^\ddagger is less than 0.013 eV.

intervals calculated from the full posterior distribution for seven different breaking speeds that span approximately 2 orders of magnitude in breaking speed.

All three parameters can be reliably estimated, free of the crippling correlation effects that plague MLE approaches, and with remarkably tight credibility intervals. Both the free energy barrier and the shape of the free energy surface are largely independent of the stretching speed. This is as expected because they underpin and determine the breaking kinetics in the first place and, per eq 1, are constants that are independent of force by construction. We note that our estimates do, however, show a statistically significant positive correlation of ΔG^\ddagger to the breaking speed, showing that the breaking speed does affect the free energy barrier, varying \sim 50 meV from the center speed of 1.20 nm/s in either direction. The resulting uncertainty is, however, an order of magnitude lower than in previous attempts to obtain ΔG^\ddagger , as discussed below. The shape of the free energy landscape (ν) is cusp-like ($\nu = \frac{1}{2}$), as opposed to linear cubic, $\nu = \frac{2}{3}$), regardless of the breaking speed. In terms of the distance to the transition state (x^\ddagger), we find that it increases with the breaking speed. We interpret this in the context of break junction experiments, where the coordination of the Au atoms sensitively determines their bond strength. The reaction coordinate is thus expected to include a sequence of complex rearrangements of the atoms in the tips to attain the most stable configuration, as the wire is traveling along the lowest energy pathway, and these rearrangements are

expected to depend on the applied force and thus the breaking speed (see the Supporting Information for more details).

In summary, the results of our Bayesian estimation demonstrate unambiguously that we can obtain robust estimates of all relevant kinetic parameters for bond rupture in atomic point contacts. Moreover, a major advance of this work is that only two junctions need to be measured for any system: one at an appropriately slow speed to establish k_0 and one at a convenient higher speed to obtain the estimates of x^\ddagger , ΔG^\ddagger , and ν . This contrasts with other methods^{12,13} where many junctions need to be measured to obtain estimates of the relevant kinetic parameters, a process that takes many days for MCBJ experiments. This is a vast improvement over the requirements for obtaining bond rupture kinetics in single-molecule transport or atomic point contact measurements, adding a new dimension to the physics that may be routinely observed in break junctions. In essence, it is enabled by using complete distributions rather than single point measures such as most likely values of lifetimes. In what follows, we discuss the physical meaning of the parameters retrieved and compare them to previous estimates and various theoretical models.

Despite intense interest and recent progress to go beyond average values in break junction experiments by understanding the shape of the complete histogram,^{1,2} there remain significant challenges e.g. in extracting microscopic information from lifetime histograms. For lifetime histograms, the milliseconds to seconds time scale of break junction measurements is significantly slower than the atomic-scale relaxation times of the junction under the stress of stretching. Because of this separation in time scales, molecular dynamics (MD) simulations cannot readily provide microscopic insight into the experimentally relevant temporal evolution of the junction during stretching, and the interpretation of the experimental lifetime distributions is thus usually limited to single point measures such as the average or most likely value. This leaves both the information content of the distribution unclear and by necessity therefore does not reflect the full physics at play. To determine the free energy of bond breaking more accurately, we suggest that the practice of summarizing the lifetime distribution through single point measures needs to be reassessed. Instead, all the data that determine the shape of the histogram should be used to capture the physics of kinetic-force-based junction rupture. It is due to this contrast that our approach can meaningfully estimate kinetic parameters from a 1D model that yields the full lifetime distribution. Naturally, the underlying model assumptions require discussion. We first carefully consider the impact of the experimental technique on the measurement. This matters because real measurements deviate in meaningful ways from the idealized description of pulling experiments, and the consequences must be included properly. Second, we consider alternative theoretical models that have been used in the past to understand lifetimes in breaking kinetics. Finally, we put the parameters estimated from our measurements and our approach into context with what is already known.

Arguably, the most important aspect determining the lifetime is the arrangement of the atoms in and near the junction during the process of stretching the wire. It is well-known from experiment that suspended Au nanowires under an external force tend to form one atom thick constrictions whose contact conductance is approximately 1 G₀.¹⁴ Surprisingly, MD simulations of gold nanowires breaking under external force show the tendency to form one atom thick

chains ranging from 2–5 atoms in length.^{15,16} This peculiar behavior suggests that the bonds of incompletely coordinated Au atoms are considerably stronger than fully saturated bonds in the bulk.

This is supported by the previous experimental results: Rubio-Bollinger et al. performed experimental force measurements on atomic gold chains with an STM-based force sensor at 4 K, supplemented by *ab initio* calculations.¹⁷ Remarkably, the simulations showed that the largest atomic displacements after the formation of the Au chain take place in the bulk of the contact near the chain ends and not in the chain itself. Furthermore, for short chains (1–2 atoms in length), the experimental chain stiffness can vary by up to a factor of 3 due to the elasticity of the nanostructure, mainly determined by the compliance of the neighboring atoms in the bulk wire near the chain ends.

From this, we reason that there are at least two severe consequences on the measured lifetimes that will necessarily broaden their distributions. The first is the variation of the Au chain length. When Au atoms near the apex are incorporated into a chain, this induces large irreversible force relaxations which must be compensated by additional stretching of the junction, as shown by Rubio-Bollinger et al. Hence, not only will the apparent breaking distance, L , be longer, but the time to rupture is also longer than that of the idealized junction because the latter does not need to undergo major relaxations before rupture.

The second consequence is that the stochastic geometric arrangement of the neighboring Au atoms near the nanowire ends is what determines the free energy barrier. It is clear from the exponential dependence of the breaking rate on the free energy barrier for breaking in eq 1 that slight changes in this barrier height can lead to massive changes in lifetime. This reasoning is supported by calculations by Todorov et al. on gold chains, who show that a change of only 0.2 eV in the barrier will change the lifetime by 5 orders of magnitude.¹⁸

To properly account for these consequences of break junction measurements, there must be a microscopic theory of breaking kinetics that specifies the underlying free energy surface along the pulling direction, to which our experimental lifetimes are sensitive. We show what kind of meaningful microscopic theory is suitable for capturing the essential aspects of break junction dynamics by first considering alternative theoretical models that have been used in the past to understand lifetimes in breaking kinetics and comparing them to the model we suggest instead.

Kramers' treatment of chemical reactions under external bias F in terms of Brownian escape from a single potential well provides a sound definition of a scalar reaction coordinate x and results in a generalized Arrhenius law for the lifetime:

$$\tau = \tau_D e^{(\Delta G^\ddagger - Fx^\ddagger)/k_B T} \quad (4)$$

where τ_D is the diffusion relaxation time which drives thermally activated escape, τ is the measured lifetime, ΔG^\ddagger is the free energy barrier, and x^\ddagger is the distance to the transition state.¹⁹

Kawai and co-workers showed that by measuring τ in an MCBJ at zero applied force, eq 4 can be used to estimate the free energy barrier.¹² However, this result was derived with a somewhat crude approximation of the underlying free energy surface (i.e., only considering a small window to integrate near the maximum of the potential barrier, rather than integrating a full functional form). The nonlinear dependence of lifetime on

free energy implies a more complex relationship between the experimentally observed parameter τ and the desired ΔG^\ddagger . Moreover, eq 4 alone cannot provide a theoretical prediction of the lifetime distribution, much less what is contributing to the shape. Though this simple model provides the basis for linking the lifetime and free energy for the reaction, a more comprehensive theory is needed that also captures the nature of the free energy landscape.

A more sophisticated model was proposed by Bell,⁵ who suggested that for the case where many bonds contribute to the barrier, the rate constant needs to be modified to include the amount of force per bond, i.e., $k_0 e^{Fx^\ddagger/k_B T N_b}$, where N_b is the number of bonds and $k_0 = \frac{1}{\tau_D} e^{-\Delta G^\ddagger/k_B T}$. This provides a better reflection of junction breaking compared with that of Kramers' theory, which only loosely defines the system as particle collisions. Bell provides crucial insight that microscopic bond properties determine the macroscopic forces required to rupture.

Tao et al. took advantage of Bell's theory to estimate the natural lifetime, $\tau_{\text{off}} = \frac{1}{k_0}$, in an STM-BJ experiment on Au and molecular junctions.^{13,20} However, while the power of Bell's equation is its generality, the expression is valid only for diffusive barrier crossing in the limit of small forces, restricting it to a limited range of breaking scenarios. Furthermore, Bell's expression does not consider the influence of a well-defined free energy surface that is coupled to the harmonic pulling potential, focusing instead only on x^\ddagger . Consequently, the underlying free energy surface is insufficiently characterized by only a single parameter, x^\ddagger , leaving the height of the free energy barrier, ΔG^\ddagger , impossible to estimate without reverting to simplistic models or including *ad hoc* assumptions.

In comparison to the theory developed by Dudko et al. which *does* specify a potential energy surface and which underpins our Bayesian estimation of breaking kinetics, it will become clear just how important this specification is when the parameters estimated from our measurements and our approach are put into context with previous estimates. Following Kawai et al. and using eq 4 to estimate the free energy barrier when $F = 0$, $\tau_D = 3.5 \times 10^{12}$ s, and transforming the measured Au lifetime distribution into a free energy barrier distribution yields a distribution centered at ~ 0.80 eV with a half-width of ~ 0.1 eV.¹² Alternatively, one may use $E_b = \frac{1}{2} F_b L$, where E_b is the energy barrier, F_b is the maximum amount of force required to break a Au–Au bond, and L is the breaking distance over which the bond can be stretched from the equilibrium bond length before breakdown. F_b , measured by an atomic force microscope (AFM) on gold chains, is 1.5 ± 0.3 nN.¹⁷ L , which is analogous to the distance to the transition state, x^\ddagger , may be determined by measuring the breaking length at extreme stretching speeds in either an MCBJ or STM-BJ setup. It is broadly distributed with a most probable value of ~ 0.17 nm. Note that the Au–Au breaking distance, L , also defined as the distance between the equilibrium bond length and the stretched bond length just before rupture, has been reported in transmission electron microscopy (TEM),^{7,21,22} MCBJ,^{12,23,24} STM-BJ¹³ experiments, MD,¹⁵ *ab initio* molecular dynamics (AIMD),²⁵ and tight binding molecular dynamics simulations²⁶ of Au chains breaking to have a range of 0.02–0.30 nm. Using the entire breaking distance distribution reported by Tao et al. yields $E_b = 0.82 \pm 0.45$ eV.¹³

The uncertainty in the above estimates of the free energy barrier is rather large and is due to several factors: First, the lifetime and breaking length distributions are broadened by both gold chaining and the stochastic geometric arrangement of the Au atoms in the nanowire, which directly governs the free energy barrier. Second, the statistical analysis of the broadened lifetime and breaking length distributions, based on a theoretical treatment that does not account for the specific nature of the free energy surface, compounds the uncertainty in the estimates. As a result, the free energy barrier is systematically overestimated and is burdened with large uncertainties.

In contrast, our model, though one-dimensional, requires fewer assumptions and is based on a treatment that specifies the underlying free energy surface. This is justified because experimental lifetimes are quite sensitive to the fact that the free energy surface needs to be specified by more than just x^\ddagger . Most importantly, and as a major innovation of this work, we combine this with a powerful Bayesian approach to make maximal use of *all* the measured data to provide robust estimates, where standard MLE techniques fail. This allows us to reliably invert experimental data and retrieve previously inaccessible or widely uncertain parameters for the kinetics of bond rupture.

In conclusion, we have shown that to extract relevant electromechanical and physically meaningful junction properties from lifetime histograms, summarizing the lifetime distribution through single point measures needs to be reassessed. Instead, all of the data and thus the full shape of the lifetime histogram should be used to capture the physics of junction breaking in atomic point contact measurements. When considering the impact of the MCBJ experimental technique on the measurement of Au–Au lifetimes carefully, two new necessary innovations are called for in the analysis of the lifetime data: First, a theoretical treatment that specifies the underlying free energy surface by more than just x^\ddagger . This is needed because experimental break junction data are sensitive to the stochastic geometric arrangement of the neighboring Au atoms near the nanowire ends, which determines the free energy barrier. Second, the adoption of Bayesian fitting procedures which makes maximal use of *all* the measured data. This is crucial because standard MLE techniques that rely on single point measures and/or binning the data can lead to overestimation with large uncertainties or may even completely fail, as in the case of fitting the experimental lifetime distribution to [eq 2](#). In the context of break junction experiments we think it would be interesting to compare the estimated kinetic parameters inferred from data generated from the same experimental junction in an MCBJ apparatus that can measure both forces and lifetimes to explore what microscopic detail may be learned by comparing the two observables.

These lessons apply more broadly to many other experimental approaches that rely on the interpretation of broadly distributed stochastic data. Clearly, our approach can be used to assess bond rupture dynamics in single-molecule transport measurements, where our results may isolate parameters needed for the theory developed by Mejia without the need for making complementary force measurements. This would be an important advance that reduces the experimental effort needed to test the theory of conductance histograms and provide internally consistent data. Applications to force measurements in biophysics also benefit from the proposed framework. Finally, we expect that entirely different physical

scenarios with inherently stochastic data that yield broad, asymmetric distributions and for which analytical models of the distribution may be developed will be amenable to the Bayesian approach in our work.

■ ASSOCIATED CONTENT

Data Availability Statement

Code for the Bayesian statistical calculations is available for free online at https://github.com/LabMonti/BayesianAnalysis_GoldBreakingData.

SI Supporting Information

The Supporting Information is available free of charge at <https://pubs.acs.org/doi/10.1021/acs.jpcllett.3c02643>.

Additional complications and consequences of the break junction architecture, testing the Bayesian methodology, and experimental methods ([PDF](#))

Transparent Peer Review report available ([PDF](#))

■ AUTHOR INFORMATION

Corresponding Author

Oliver L. A. Monti — Department of Chemistry and Biochemistry and Department of Physics, The University of Arizona, Tucson, Arizona 85721, United States;
✉ orcid.org/0000-0002-0974-7253; Phone: +520 626 1177; Email: monti@arizona.edu

Author

Dylan Dyer — Department of Chemistry and Biochemistry, The University of Arizona, Tucson, Arizona 85721, United States; ✉ orcid.org/0000-0002-2747-9301

Complete contact information is available at:
<https://pubs.acs.org/10.1021/acs.jpcllett.3c02643>

Notes

The authors declare no competing financial interest.

■ ACKNOWLEDGMENTS

The authors acknowledge support from the National Science Foundation award no. DMR-2225369 as well as the Alfred P. Sloan Foundation award no. G-2020-12684. Plasma etching was performed in part using a Plasmatherm reactive ion etcher acquired through an NSF MRI grant, award no. ECCS-1725571, as well as an AGS reactive ion etcher located in the Micro/Nano Fabrication Center at the University of Arizona. Bayesian statistical calculations were performed using High-Performance Computing (HPC) resources supported by the University of Arizona TRIF, UITS, and RDI and maintained by the UA Research Technologies department. Quality control was performed using a scanning electron microscope in the W. M. Keck Center for Nano-Scale Imaging in the Department of Chemistry and Biochemistry at the University of Arizona with funding from the W. M. Keck Foundation Grant. A special thanks goes to Koen Visscher and Chris Jarzynski for their wonderful collaborative spirit and invaluable guidance on theoretical background in force spectroscopy. We also thank Manny Smeu and Hashan Peiris for insightful discussions.

■ REFERENCES

- (1) Mejia, L.; Cossio, P.; Franco, I. Microscopic theory, analysis, and interpretation of conductance histograms in molecular junctions. *Nat Commun* **2023**, *14*, 7646.

(2) Li, Z.; Mejía, L.; Marrs, J.; Jeong, H.; Hihath, J.; Franco, I. understanding the conductance dispersion of single-molecule junctions. *J. Phys. Chem. C* **2021**, *125*, 3406–3414.

(3) Dudko, O.; Hummer, G.; Szabo, A. intrinsic rates and activation free energies from single-molecule pulling experiments. *Phys. Rev. Lett.* **2006**, *96*, No. 108101.

(4) Zhan, C.; Wang, G.; Zhang, X.; Li, Z.; Wei, J.; Si, Y.; Yang, Y.; Hong, W.; Tian, Z. single-molecule measurement of adsorption free energy at the solid–liquid interface. *Angew. Chem., Int. Ed.* **2019**, *58*, 14534–14538.

(5) Bell, G. I. models for the specific adhesion of cells to cells: a theoretical framework for adhesion mediated by reversible bonds between cell surface molecules. *Science* **1978**, *200*, 618–627.

(6) Izrailev, S.; Stepaniants, S.; Balsara, M.; Oono, Y.; Schulten, K. molecular dynamics study of unbinding of the avidin-biotin complex. *Biophys. J.* **1997**, *72*, 1568–1581.

(7) Rodrigues, V.; Ugarte, D. real-time imaging of atomistic process in one-atom-thick metal junctions. *Phys. Rev. B* **2001**, *63*, No. 073405.

(8) Evans, E. probing the relation between force—lifetime—and chemistry in single molecular bonds. *Annu. Rev. Biophys. Biomol. Struct.* **2001**, *30*, 105–128.

(9) Evans, E.; Ritchie, K. dynamic strength of molecular adhesion bonds. *Biophys. J.* **1997**, *72*, 1541–1555.

(10) Hummer, G.; Szabo, A. kinetics from nonequilibrium single-molecule pulling experiments. *Biophys. J.* **2003**, *85*, 5–15.

(11) Berger, J. O.; Bernardo, J. M. on the development of the reference prior method. *Bayesian Stat.* **1992**, *4*, 35–60.

(12) Tsutsui, M.; Shoji, K.; Taniguchi, M.; Kawai, T. formation and self-breaking mechanism of stable atom-sized junctions. *Nano Lett.* **2008**, *8*, 345–349.

(13) Huang; Chen, F.; Bennett, P. A.; Tao, N. J. single molecule junctions formed via au–thiol contact: stability and breakdown mechanism. *J. Am. Chem. Soc.* **2007**, *129*, 13225–13231.

(14) Agrait, N. quantum properties of atomic-sized conductors. *Phys. Rep.* **2003**, *377*, 81–279.

(15) Bahn, S. R.; Jacobsen, K. W. chain formation of metal atoms. *Phys. Rev. Lett.* **2001**, *87*, No. 266101.

(16) da Silva, E.; da Silva, A.; Fazzio, A. how do gold nanowires break? *Phys. Rev. Lett.* **2001**, *87*, No. 256102.

(17) Rubio-Bollinger, G.; Bahn, S. R.; Agrait, N.; Jacobsen, K. W.; Vieira, S. mechanical properties and formation mechanisms of a wire of single gold atoms. *Phys. Rev. Lett.* **2001**, *87*, No. 026101.

(18) Todorov, T. N.; Hoekstra, J.; Sutton, A. P. current-induced embrittlement of atomic wires. *Phys. Rev. Lett.* **2001**, *86*, 3606–3609.

(19) Kramers, H. A. brownian motion in a field of force and the diffusion model of chemical reactions. *Physica* **1940**, *7*, 284–304.

(20) Huang; Xu; Chen, di; Ventra, M.; Tao, N. J. measurement of current-induced local heating in a single molecule junction. *Nano Lett.* **2006**, *6*, 1240–1244.

(21) Ohnishi, H.; Kondo, Y.; Takayanagi, K. quantized conductance through individual rows of suspended gold atoms. *Nature* **1998**, *395*, 780–783.

(22) Kizuka, T. atomic configuration and mechanical and electrical properties of stable gold wires of single-atom width. *Phys. Rev. B* **2008**, *77*, No. 155401.

(23) Smit, R. H. M.; Untiedt, C.; Yanson, A. I.; van Ruitenbeek, J. M. common origin for surface reconstruction and the formation of chains of metal atoms. *Phys. Rev. Lett.* **2001**, *87*, No. 266102.

(24) Untiedt, C.; Yanson, A. I.; Grande, R.; Rubio-Bollinger, G.; Agrait, N.; Vieira, S.; van Ruitenbeek, J. M. calibration of the length of a chain of single gold atoms. *Phys. Rev. B* **2002**, *66*, No. 085418.

(25) Okamoto, M.; Takayanagi, K. structure and conductance of a gold atomic chain. *Phys. Rev. B* **1999**, *60*, 7808–7811.

(26) Hasmy, A.; Rincón, L.; Hernández, R.; Mujica, V.; Márquez, M.; González, C. on the formation of suspended noble-metal monatomic chains. *Phys. Rev. B* **2008**, *78*, No. 115409.